Menon, L. R., McIlroy, D., Liu, A., & Brasier, M. D. (2016). The dynamic influence of microbial mats on sediments: fluid escape and pseudofossil formation in the Ediacaran Longmyndian Supergroup, UK. *Journal of the Geological Society*, *173*(1), 177-185. [2015-036]. https://doi.org/10.1144/jgs2015-036

The dynamic influence of microbial mats on sediments: fluid escape and pseudofossil formation in the Ediacaran Longmyndian Supergroup, UK

LATHA R. MENON[1*], DUNCAN MCILROY[2], ALEXANDER G. LIU[3], and MARTIN D. BRASIER[1,2 †]

[1]Department of Earth Sciences, University of Oxford, South Parks Road, Oxford, OX1 3AN, UK

[2]Department of Earth Sciences, Memorial University of Newfoundland, St John's, NL, A1B 3X5, Canada

[3]School of Earth Sciences, University of Bristol, Life Sciences Building, 24 Tyndall Avenue, Bristol BS8 1TQ

[†]Deceased

**Corresponding author (e-mail: menon891@btinternet.com)*

No. of words: 2970 incl. references, plus 10 figures (estimated length 6.7 pages overall)

Abbreviated title: Dynamic influence of microbial mats

Abstract: Microbial mats are thought to have been widespread in marine settings before the advent of bioturbation, and the range of their influence on sediments is gradually becoming recognized. We propose that mat sealing can dynamically affect pore-water conditions and enable the build-up of overpressure that can drive dewatering and degassing to produce a suite of atypical fluid-escape features. Finely bedded silty and sandy laminae from the *c*. 560 Ma Burway Formation of the Longmyndian Supergroup, Shropshire, England, reveal evidence for sediment injection, including disrupted bedding, clastic injections, sill-like features, and sediment volcanoes at sub-millimetre scale. These features are associated with crinkly laminae diagnostic of microbial matgrounds. Matground-associated fluid injection can explain the formation of several types of enigmatic discoidal impressions, common in marginal marine facies of this age, which have previously been attributed to the Ediacaran macrobiota. Serial grinding of Longmyndian forms previously described as *Medusinites* aff. *asteroides* and *Beltanelliformis* demonstrate that such discoidal features can be fully explained by fluid escape and associated load structures. Our observations emphasize the non-actualistic nature of shallow-marine Ediacaran sediments. Matground-associated sediment injection features provide a new insight into the interpretation of Proterozoic rocks and the biogenicity of their enigmatic discoidal markings.

Supplementary material: A document containing further images of fluid escape and loading features observed in the upper Burway Formation at Ashes Hollow, together with an annotated diagram of features appearing in one typical vertical cross-section, is available at www.geolsoc.org.uk/SUP00000.

The abundance and importance of microbial mats on the Ediacaran seafloor has been widely discussed (e.g. McIlroy & Walter 1997; Seilacher 1999; Gehling 1999; Liu *et al.* 2011). Microbially mediated sedimentary structures resulting from seafloor biostabilization and build-up of decay gases below matgrounds (e.g. gas domes, “sponge pore” fabrics) are now well characterized (see Gerdes *et al.* 1994; Noffke 2010; Schieber *et al.* 2007). Most studies have focused on structures formed in association with cyanobacterial mats in intertidal settings, but many of the fundamental properties required to generate such forms are inferred to apply to all types of microbial mat.

Here we document features from the Ediacaran Longmyndian Supergroup, Shropshire, England that are considered to arise from the dynamic influence of mat sealing on unconsolidated fluid-rich sediment. We also demonstrate that some of the enigmatic sedimentary structures commonly observed within late Ediacaran successions - and interpreted as fossils - should now be re-interpreted in terms of mat-driven processes. Our model provides a physical explanation for at least three forms of discoidal impression observed in these strata: *Medusinites* aff. *asteroides*, *Beltanelliformis brunsae* Menner, and *B. minutae* (cf. McIlroy *et al.* 2005).

Lithology, palaeoenvironmental context, and surface features

The specimens discussed here were collected from a disused quarry in Ashes Hollow, from horizons approximately 75 m below the Cardingmill Grit, close to the top of the Burway Formation, Stretton Group, Longmyndian Supergroup (Fig. 1). The discoidal fossils occur in heterolithic facies of mudstone to fine siltstone interlaminated with fine sandstone (Pauley 1986; McIlroy *et al.* 2005). The lamination, typically <0.2–1 mm in width, is mostly plane parallel, with some cross-lamination and contorted laminae in places stretching a few centimetres, with occasional small microfaults. Grains include a significant volcanic and plutonic component from the Uriconian Volcanic Complex underlying the Stretton Group (Pauley 1986, 1990). The chloritic mudstone and siltstone are greenish-grey in hand specimen, while the amalgamated sandstone is dark brown due to the presence of haematite (Pauley 1986). Intermittent thin (<0.3 mm), white laminae have previously been identified as hosting mineralized microbial mats preserved in a white aluminosilicate mineral (Callow & Brasier 2009). The colour contrast between the mudstone and inter-laminated sandstone allows sub-millimetric sediment fabrics to be studied in polished vertical section. The age of the Burway Formation is currently constrained by U/Pb SHRIMP geochronology to between 566.6 ±2.9 Ma in a lapilli tuff at the base of the underlying Stretton Shale Formation, and 555.9 ± 3.5 at the top of the stratigraphically higher Lightspout Formation (Compston *et al.* 2002).

Sole surfaces of some Ashes Hollow beds are covered with millimetre-scale mounds, typically of 2 mm diameter, and pinhead-like protuberances (“pimples”), with rimless counterpart pits on the tops of underlying beds (Fig. 2a–c; Table 1). Shallow (0.5 mm depth), rimless discoidal depressions, generally larger and lacking the sharp edges of the counterpart pits, are also found on top surfaces (Fig. 2d; Table 1). Discoidal forms were first noted in the Burway and Synalds Formations of the Longmyndian Supergroup in the 19^{th} century (Salter 1856; described in Callow *et al.* 2011). They were originally inferred to be biological structures of simple animals (Salter 1856; Darwin 1859), but this interpretation has subsequently been much debated (e.g. Cobbold 1900; Pauley 1986, 1990; Toghill 2006; Liu 2011). The possible interpretation of circular impressions as rain-pits, that would in any case be rimmed, is ruled out by the recognition of subaqueous deposition of the Burway Formation (Pauley 1990). The discoidal forms have more recently been regarded as fossils of simple Ediacaran organisms belonging to form taxa *Medusinites* aff. *asteroides*, *Beltanelliformis brunsae*, and *B. minutae* (McIlroy *et al.* 2005).

The most distinctive discoidal fossil from the Burway Formation is *Medusinites* aff. *asteroides,* a blister-like mound of 1–6 mm diameter, sometimes with a central boss, locally found in large numbers on the soles of beds (Fig. 2a). *Medusinites* mounds in cross-section are typically filled with dark sandy sediment, sometimes with a tube-like extension above, which was thought to represent the passage of either gas or an organism (Cobbold 1900). Since gas-escape structures are rarely preserved in this way, McIlroy *et al.* (2005) tentatively concluded that *Medusinites* may be a trace fossil.

Microbial-mat-associated “elephant skin”, wrinkle textures, and thread-like markings are also seen on surfaces of Stretton Group rocks in association with discoidal markings (McIlroy *et al.* 2005; Fig. 2e). Widespread filamentous microfossils consistent with mat fabrics have also been observed from the Burway and Lightspout Formations (Peat 1984; Callow & Brasier 2009).

Methodology

We investigated serial polished vertical cross-sections through hand samples bearing *Medusinites,* “pimples”, and the *Beltanelliformis*-like shallow depressions, to examine the discoidal structures, the potential trace fossils, and the associated matground fabrics. Hand specimens were first cut in a series of slices of 1 cm depth and the cross-sections polished, to form a general impression of the features in cross-section. Individual discoidal specimens were then hand-ground with 15-μm carborundum powder on a glass plate, and photographed at intervals of 1 minute, with the removal of ~0.1 mm of rock between grinds, for detailed study, and at intervals of 5 minutes, with the removal of ~0.25 mm of rock between grinds, for confirmation and checking of features. This hand-grinding process proved to be sufficient for the interpretation of the features.

In addition, two specimens of the more complex lobate form, and one *Medusinites*, were subjected to mechanical grinding to facilitate detailed three-dimensional visualization. These samples were ground on a Logitech LP30 lapping and optical polishing machine at the Oxford University Museum of Natural History. Specimens were embedded in resin, and ground at 20 μm intervals. Photographs were taken after each grinding stage following wetting of the specimens with water to increase image contrast. The SPIERS software package (Sutton *et al*. 2012) was used to align and edit the image sequences, and to reconstruct virtual 3D models of the specimens.

Upper Burway Formation rocks in vertical section

Examination of beds with crinkly laminae in vertical cross-section revealed a suite of sedimentary features that disrupt laminae at scales of < 0.5 to 10 mm, of which the columns of sandstone above *Medusinites* form only a part (Fig. 3a; Table 1). These features include irregular, often widening, sub-vertical columns of sandstone that have horizontal branches penetrating into associated laminae (Fig. 3b). Larger areas of vertical disruption encompassing over 2 cm of sediment thickness (Fig. 3c), with displaced and locally discontinuous laminae and fragments of green mudstone laminae within the zone of disruption, are associated with strikingly crinkled whitish sedimentary laminae that would be conventionally attributed to microbial matgrounds (Noffke 2010). Such white laminae have previously been shown to contain intermeshed microbial filaments (Callow & Brasier 2009). Serial grinding through one such area demonstrated that the disrupted region was less than 5 mm wide. Moreover, the laminae cut by the disturbance do not show systematic displacement; some laminae are displaced, others simply discontinuous. This contrasts with the small microfaults observed in these sections, and indicates that the feature results from localized soft-sediment deformation. Where the sediment columns reach bedding surfaces (e.g. Fig. 3c and d), they are associated with small apex-up cones and craters of 1–5 mm in diameter and 0.5–1.5 mm height (Fig. 3e).

Petrographic study of these lithologies provides substantial evidence for the former presence of widespread microbial mats, including crinkled laminae, intermeshed filaments angled at approximately 45° to bedding, trapped and bound sediment grains, and the preferential alignment of muscovite and other elongated grains within the matground facies (cf. Noffke 2010; Figs 4, 5; see also Peat 1984; Callow & Brasier 2009).

All simple mound-like *Medusinites* examined in cross-section by serial grinding reveal a protruding mound that is wholly filled with dark sandstone of the same lithology as the surrounding sandstone laminae, frequently with a sub-vertical columnar extension (Fig. 6a and b). This sediment column distorts and cuts mudstone laminae above the discoidal impression, and typically terminates at an overlying sandstone bed (Fig. 6b). *Medusinites* with a central boss have a partial fill of sandstone, encompassing the boss and widening laterally a little above the centre of the mound (Fig. 6c and d). Negative counterparts of *Medusinites* found on the tops of beds (Fig. 2b) are underlain by irregular dark-coloured sandstone structures that intersect the centre of the pit (Fig. 6e and f). These sandstone features are of the same lithology and texture as the surrounding sandstone laminae. Cross-sections through the pimple-like impressions on bed soles attributed to *B. minutae* (McIlroy *et al.* 2005; Fig. 2a and c) show narrow columnar features (Fig. 6g and h).

A tetra-lobate form, comprising a mound divided into four lobes by shallow radial grooves extending from the central pimple (Fig. 2a) was also examined by serial grinding. This form is found in association with normal, rounded *Medusinites* in patches on some bedding planes, and has been regarded as a variant of *Medusinites* (Pauley 1986). The tetra-lobate form appears to represent the most symmetrical example of a wider tendency towards lobe formation in *Medusinites*. Many *Medusinites*, up to ~20% of specimens in some patches, show between 3 and, more typically, 5 poorly formed lobes. In cross-section the lobed forms have sandstone fills very similar to those of non-lobed forms of *Medusinites* (cf. Fig. 6c and d) and the lobes are found to be composed of un-laminated mudstone with an admixture of 20–40% sandstone (Fig. 7a–h).

Shallow depressions on the tops of beds from the locality with *Medusinites* (Fig. 2d), previously described as *Beltanelliformis brunsae* (McIlroy *et al.*, 2005), were also serially ground, both in vertical cross-section and parallel to bedding, revealing roughly apex-down conical structures composed of dark sandstone, again of the same lithology and texture as the surrounding sandstone laminae (Fig. 8a–c; Table 1). These conical structures do not reach the impression-bearing surface but terminate just below it, as a sill-like spread with central depression (Fig. 8c). Such conical structures are seen in vertical cross-section to extend downwards as meandering, tapering columns, often linking the conical structure to a sandstone bed below (Fig. 8a, b and d).

Interpretation

The features observed in our material strongly suggest small-scale injection of sand slurries. Features suggesting fluid escape processes include highly disturbed and torn laminae, fragments of green mudstone and white matgrounds entrained in lamina-cutting features filled with sandstone, and small sand volcanoes (Fig. 3c–e; Fig. 4a; Fig. 6b, h). The sediment deformation fits the pattern of injected (non-neptunian) clastic dykes and sills (cf. Dżułyński & Walton 1965), but at a much smaller scale. Clastic dykes occur at scales of centimetres to many metres and are usually associated with slumping and tectonic instability (Smith & Rast 1958). Dykes and sills resulting from loading and sediment compaction are also known (e.g. Harazim *et al.* 2013), but these too are larger in scale. Small-scale dewatering structures have been reported from regions of rapid sedimentation in some Ediacaran deposits (e.g. Farmer *et al.* 1991). There is no evidence of slumping or rapid sedimentation in the upper Burway Formation. Apart from the small-scale disruptions, and occasional examples of low-angle cross-lamination, the laminae are plane parallel and suggest a low energy, shallow-marine environment (Pauley 1986, 1990). We propose that the very small-scale (predominantly millimetric) fluid injection features result from the influence of the microbial mats.

The effects of microbial mats on sealing and gas exchange in intertidal settings have previously been noted (Gerdes *et al.* 1994; Noffke 2010; Schieber et al. 2007). In fully marine conditions, microbial mat sealing can also affect pore pressure in unconsolidated sediments, allowing the build-up of overpressure in sub-matground sediments (Harazim *et al.* 2013). The suite of features described here is considered to result from the dewatering of pore-water-rich unconsolidated sediments, driven by sediment loading and the sealing effect of microbial mats. Sediment injection, which occurs during compaction of sediments, requires the rise of pore waters at sufficient force to mobilize and entrain sediment grains, and tends to produce fluid-escape structures in fine-grained sands overlain by cohesive layers such as clay (Lowe 1975; Nichols *et al*. 1994; Frey *et al*. 2009). Here, in spite of relatively quiet and stable conditions of sedimentation, the effect of cohesive, sealing matgrounds on sediments that appear from the examples of soft-sediment deformation to have overlain pore-water rich muds would have been sufficient to produce sediment injection on a small scale. The scale may also reflect the thin sedimentary laminae involved (<0.5 mm thick), which may have limited the amount of sedimentary material available for sediment-injection during dewatering of any particular horizon.

The correlation of regions of high sediment disruption with indicators of decayed microbial matgrounds (see e.g. Fig. 4a) is consistent with mat sealing operating as a fundamental process in such sediments. In thin section, the interaction between matgrounds and porewater-rich sediment evinces the role of mats in sediment sealing and in constraining and modifying the features of mobilized sediment (Fig. 4b and c). Intermeshed mat filaments are observed to surround loading structures and are inferred to influence their shape (Fig. 4b and c). Additionally, matgrounds appear to obstruct the upward injection of sediment columns (e.g. Fig. 6d; Fig. 7b, c, f, and h). Microbial metabolism and necrosis are known to result in the build-up of gas in association with matgrounds, and may form such features as gas domes and pustules on the sediment surface, some of which may burst before burial (see e.g. Gerdes 2007). The escape of such gases following sedimentation may have left paths for porewaters to subsequently follow during burial compaction.

Upward injection and spread of sand slurries resulting from mat sealing is here inferred to have caused deformation of sedimentary laminae to produce loading structures on bed soles that have previously been attributed to *Medusinites* (Fig. 9). If sand slurry is injected with sufficient force to spread at stratigraphically higher levels than the preserved discoidal impression, the injection point may be preserved as a central boss (Figs 2a, 6c). Immediate spread of the sand slurry on injection results in loading of the whole injection area, producing a smooth mound on the bed sole (Fig. 6a and b). Grinding of "Medusinites" counterparts from the Longmyndian confirms that a sandstone column extends below the centre of this structure, supporting the abiogenic injection model for creation of these features (Fig. 6e and f). Injections that rise without spreading produce isolated pimples on bed soles (and counterpart pits on underlying beds) previously identified as *Beltanelliformis minutae* (Fig. 2a and c; Fig. 6g and h). Lobe formation around the injection point in some Longmyndian "Medusinites" is a subtle feature that we suggest arises from the particular hydrostatic conditions of these fluid injection, and the rheology of the sediment at the bedding plane in question. Without knowledge of the precise conditions of fluid injection, it is difficult to investigate such features experimentally. However, the significant point here is that the irregular and widening spread of sand slurry above the lobate forms rules out the possibility that these impressions are either body or trace fossils of Ediacaran organisms. Their abiogenic origin is hereby established.

The shallow rimless depressions, formerly described as Longmyndian *Beltanelliformis brunsae* and found on some top surfaces of upper Burway Formation beds, can also be explained in terms of fluid movement and sediment loading above porewater rich unconsolidated muds, which produces the inverted conical sandstone features observed in cross-section in the underlying laminae (Fig. 8a–b). The injection of sand slurry into overlying sediment results in a small horizontal spread of sand slurry between laminae (Fig. 8c). This additional sand concentrated around the injection pipe is inferred to cause loading into the underlying unconsolidated porewater rich muds to produce an inverted cone with a central depression, causing distortion of laminae in the mudstone (Fig. 8a–b; Fig. 9). The presence of a sinking cone in a lamina just below the bedding surface causes the surface layer to drop (Fig. 8b), thereby producing the characteristic rimless depression of *B. brunsae* (Fig. 9).

Our interpretation of the Long Mynd sediments explains many of the conical, columnar, and discoidal features seen in the Burway Formation as fluid injection structures rather than trace or body fossils. The Longmyndian form of *Medusinites*, “Beltanelliformis minutae”, and the rimless depressions in the Burway Formation previously called *Beltanelliformis brunsae* can now confidently be regarded as pseudofossils.

Conclusions

This study widens the range and scale of the dynamic influence exerted by microbial mats on Ediacaran marine sediments. Microbial mats are already understood to play a key role in capturing and promoting the rapid lithification of moulds of Ediacaran organisms, leading to their being cast by unconsolidated sandy sediment from above or below (the “death mask” scenario; Gehling 1999). In that case, the movement of sediment is passive, filling the void resulting from the decay of the organism. In the model proposed here, the sediment sealing effect of microbial matgrounds is considered to have driven small-scale fluid escape and remobilization of unconsolidated sediment during the early stages of sediment dewatering close to the sediment-water interface. As a consequence, at least some of the distinctive Longmyndian discoidal markings, whose biogenicity has been debated for over a century, are hereby shown to be pseudofossils resulting from fluid-escape associated with sediment dewatering.

In many parts of the world, fossil assemblages of latest Ediacaran age are characterised not by distinctive members of the 'vendobiont' Ediacaran biota, but by circular discoidal impressions. The simplicity of circular interface impressions makes objective assessments of biogenicity difficult to prove or refute based on external morphology alone. Our study highlights the critical importance of examining ancient structures in cross-section. The small-scale mat-driven fluid injection features described here (summarized in Fig. 9), should now be sought in other matground-dominated palaeoenvironments. While such features may arise in any unconsolidated, fine sediments with microbial mat layers, both Recent and ancient, their potential for producing abiogenic discoidal structures is particularly significant for interpreting Precambrian palaeobiology, palaeoecology, and taphonomy, and consequently for our understanding of the early evolution of complex animal life. In the light of this work, the biogenicity of some of the simple circular bedding plane impressions claimed as very old fossils, such as the "Twitya discs" (Hofmann *et al.* 1990), requires careful reassessment.

We thank Kim Dunn, Jeremy Hyde, Carolyn Lewis, and Derek Siveter for technical assistance; and Aron Bowers, Richard Callow, Keith Hotchkiss, Christ Stratton, and Peter Toghill for assistance at field sites and in the collection of samples. DM acknowledges the support of the NSERC and a Canada Research Chair, and AGL acknowledges support from a Henslow Junior Research Fellowship of the Cambridge Philosophical Society, and a NERC Independent Research Fellowship [grant number NE/L011409/1]. We dedicate this paper to Professor Martin Brasier, our co-author, mentor, and friend, who died while the paper was in preparation.

References

Callow, R.H.T. & Brasier, M.D. 2009. Remarkable preservation of microbial mats in Neoproterozoic siliciclastic settings: Implications for Ediacaran taphonomic models. *Earth-Science Reviews*, **96**, 207-219.

Callow, R.H.T., McIlroy, D. & Brasier, M.D. 2011. John Salter and the Ediacaran fauna of the Longmyndian Supergroup. *Ichnos: an international journal for plant and animal traces*, **18**(3), 176-187.

Cobbold, E.S. 1900. Geology, Macro-lepidoptera and Molluscs. *In:* Campbell-Hyslop, C.W. & Cobbold, E.S. (eds) *Church Stretton Vol. 1*. L. Wilding, Shrewsbury, England, 115 pp.

Compston, W., Wright, A.E. & Toghill, P. 2002. Dating the Late Precambrian volcanicity of England and Wales. *Journal of the Geological Society, London*, **159**, 323-339.

Darwin, C.R., 1859. *On the Origin of Species by Means of Natural Selection, or the Preservation of Favoured Races in the Struggle for Life*. John Murray, London, 502 pp.

Dżułyński, S. & Walton, E.,K. 1965. *Sedimentary Features of Flysch and Greywackes*. Elsevier, Amsterdam, pp. 274.

Farmer, J., Vidal, G., Moczydlowska, M., Strauss, H., Ahlberg, P. & Siedlecka, A. 1992. Ediacaran fossils from the Innerelv Member (late Proterozoic) of the Tanafjorden area, northeastern Finnmark. *Geological Magazine*, **129**(2), 181-195.

Frey, S.E., Gingras, M.K. & Dashtgard, S.E. 2009. Experimental studies of gas-escape and water-escape structures: mechanisms and morphologies. *Journal of Sedimentary Research*, **79**, 808-816.

Gehling, J.G. 1999. Microbial mats in terminal Proterozoic siliciclastics; Ediacaran death masks. *Palaios*, **14**(1), 40-57.

Gerdes, G., Krumbein, W.E. & Reineck, H.-E. 1994. Microbial mats as architects of sedimentary surface structures. *In:* Krumbein, W.E., Paterson, D.M. & Stal, L.J. (eds) *Biostabilization of Sediments.* Bibliotheks und Informationssystem der Universitat Oldenburg, Oldenburg, Germany, p. 165-182.

Gerdes, G. 2007. Structures left by modern microbial mats in their host sediments. *In:* Schieber, J., Bose, P.K., Eriksson, P.G., Banerjee, S., Sarkar, S., Altermann, W. & Catuneau, O. (eds) *Atlas of microbial mat features preserved within the siliciclastic rock record.* Elsevier, Amsterdam, 324 pp.

Grazhdankin, D. & Gerdes, G. 2007. Ediacaran microbial colonies. *Lethaia*, **40**(3), 201-210.

Harazim, D., Callow, R.H.T. & McIlroy, D. 2013. Microbial mats implicated in the generation of intrastratal shrinkage ('synaeresis') cracks. *Sedimentology*, **60**(7), 1621-1638.

Hofmann, H.J., Narbonne, G.M. & Aitken, J.D. 1990. Ediacaran remains from intertillite beds in northwestern Canada. *Geology*, **18**, 1199-1202.

Liu, A.G. 2011. Reviewing the Ediacaran fossils of the Long Mynd, Shropshire. *Proceedings of the Shropshire Geological Society,* **16**, 31-43.

Liu, A.G., McIlroy, D., Antcliffe, J.B. & Brasier, M.D. 2011. Effaced preservation in the Ediacaran biota of Avalonia and its implications for the early macrofossil record. *Palaeontology*, **54**, 607-630.

Lowe, D.R. 1975. Water escape structures in coarse-grained sediments. *Sedimentology*, **22**, 157-204.

McIlroy, D. & Walter, M.R. 1997. A reconsideration of the biogenicity of *Arumberia banksi* Glaessner & Walter. *Alcheringa: An Australasian Journal of Palaeontology*, **21**(1), 79-80.

McIlroy, D., Crimes, T.P. & Pauley, J.C. 2005. Fossils and matgrounds from the Neoproterozoic Longmyndian Supergroup, Shropshire, UK. *Geological Magazine*, **142**(4), 441-455.

Nichols, R.J., Sparks, R.S.J. & Wilson, C.J.N. 1994. Experimental studies of the fluidization of layered sediments and the formation of fluid escape structures. *Sedimentology*, **41**, 233-253.

Noffke, N., 2010. *Geobiology: Microbial Mats in Sandy Deposits from the Archaean Era to Today*. Springer, Heidelberg, 194 pp.

Pauley, J.C. 1986. *The Longmyndian Supergroup: facies, stratigraphy and structure.* PhD thesis, University of Liverpool, 360 pp.

Pauley, J.C. 1990. Sedimentology, structural evolution and tectonic setting of the late Precambrian Longmyndian Supergroup of the Welsh Borderland, UK. Geological Society, London, Special Publications, **51**, 341-351.

Pauley, J.C. 1991. A revision of the stratigraphy of the Longmyndian Supergroup, Welsh Borderland, and of its relationship to the Uriconian volcanic complex. *Geological Journal*, **26**, 167-183.

Peat, C.J. 1984. Precambrian microfossils from the Longmyndian of Shropshire. *Proceedings of the Geologists Association,* **95**, 17-22.

Salter, J.W. 1856. On fossil remains in the Cambrian rocks of the Longmynd and North Wales. *Quarterly Journal of the Geological Society*, **12**, 246-251.

Schieber, J., Bose, P.K., Eriksson, P.G., Banerjee, S., Sarkar, S., Altermann, W. & Catuneanu, O. (eds) 2007. *Atlas of microbial mat features preserved within the siliciclastic rock record.* Elsevier, Amsterdam, 324 pp.

Seilacher, A. 1999. Biomat-related lifestyles in the Precambrian. *Palaios,* **14**(1), 86-93.

Smith, A.J. & Rast, N. 1958. Sedimentary dykes in the Dalradian of Scotland. *Geological Magazine,* **95**, 234-240.

Sutton, M. D., Garwood, R. J., Siveter, D. J. & Siveter, D. J. 2012. SPIERS and VAXML; A software toolkit for tomographic visualisation and a format for virtual specimen interchange. *Palaeontologia Electronica*, **15**(2), 1-14.

Toghill, P. 2006. *The Geology of Shropshire*, 2nd edn. The Crowood Press Ltd, Marlborough, UK, 253 pp.

FIGURE CAPTIONS

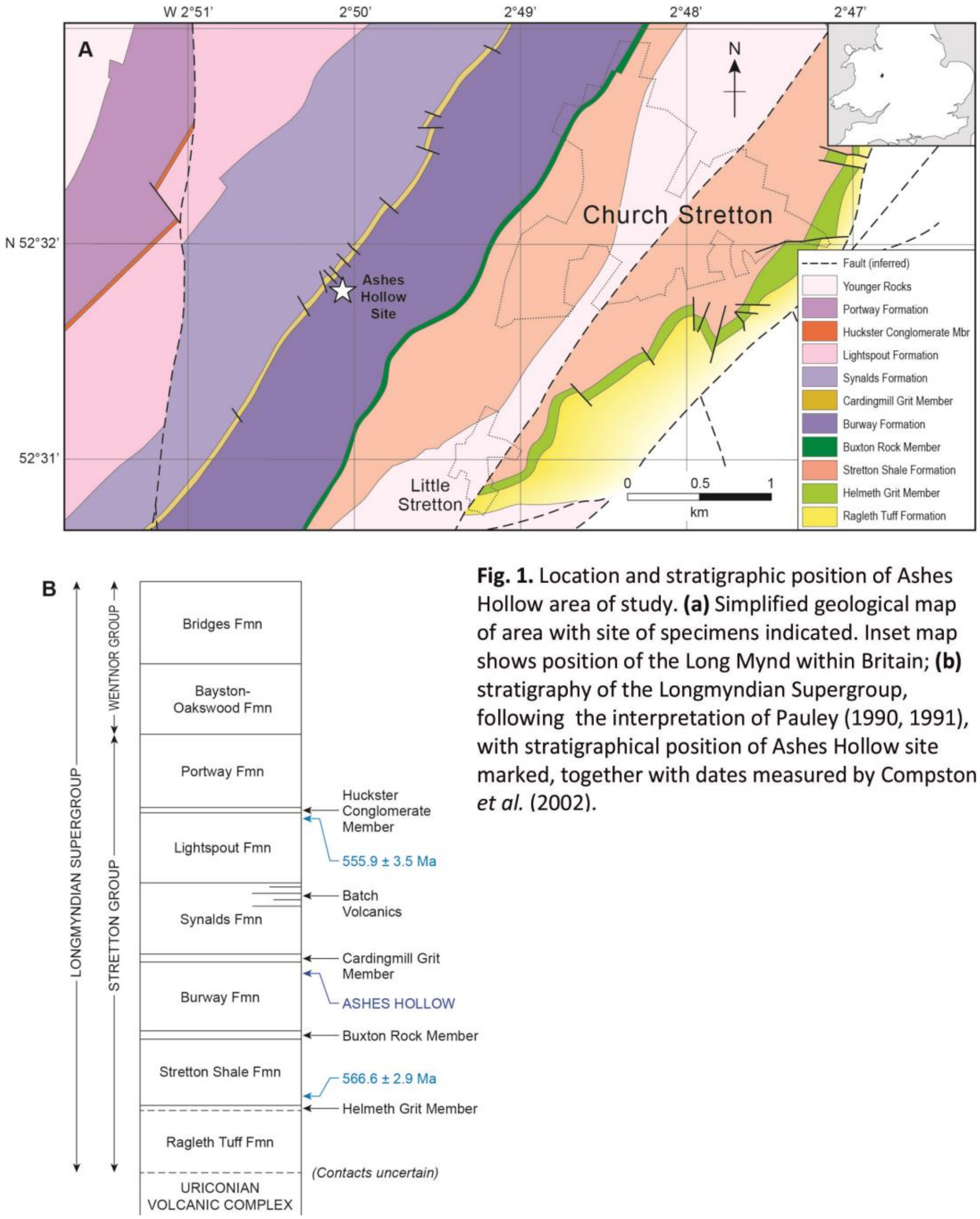

Fig. 1. Location and stratigraphic position of Ashes Hollow area of study. **(a)** Simplified geological map of area with site of specimens indicated. Inset map shows position of the Long Mynd within Britain; **(b)** stratigraphy of the Longmyndian Supergroup, following the interpretation of Pauley (1990, 1991), with stratigraphical position of Ashes Hollow site marked, together with dates measured by Compston *et al.* (2002).

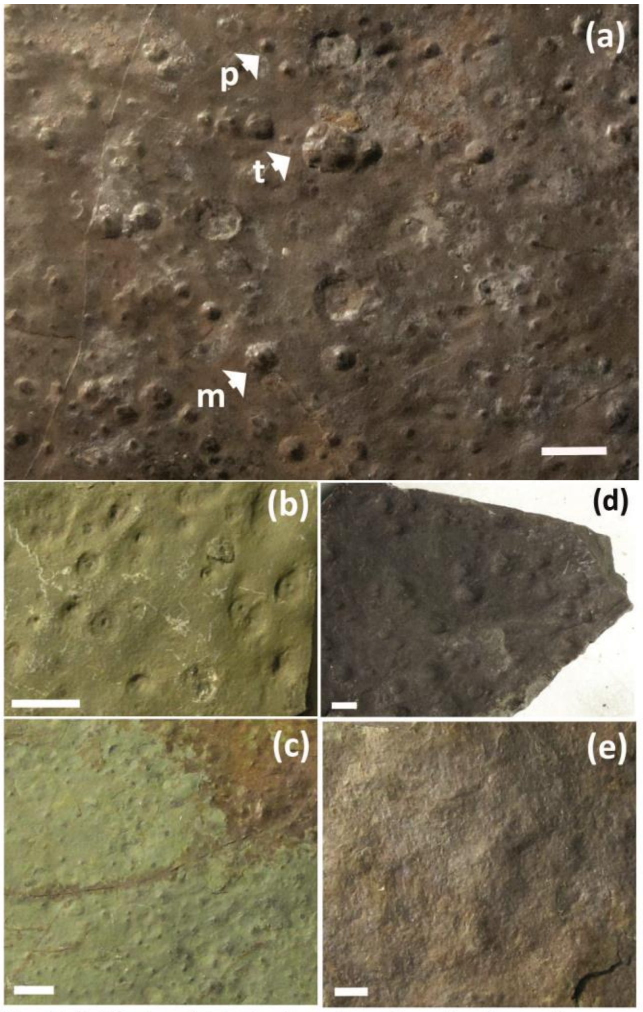

Fig. 2. **(a)** Sole of block showing abundant small Longmyndian *Medusinites* ('m'), individual pimple protrusions described as *Beltanelliformis minutae* ('p'), and occasional tetra-lobate discs ('t'); **(b)** negative epirelief counterparts of *Medusinites* on top of bed; **(c)** sole surface covered with *B. minutae;* **(d)** Shallow, rimless depressions, described as Longmyndian *B. brunsae,* on top of bed; **(e)** microbial-mat-associated texture on top surface. Scale bars: 5 mm.

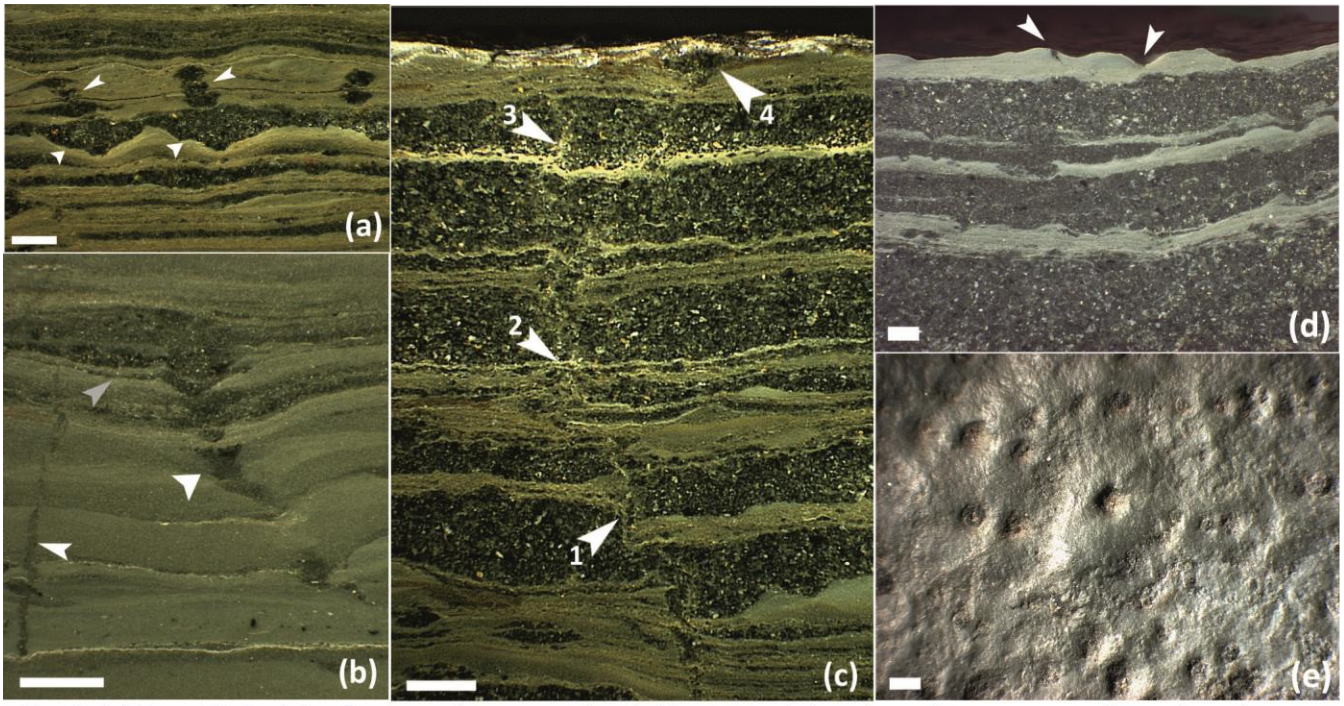

Fig. 3. (a) Two *Medusinites* in ground cross-section (wide arrows) showing columnar extensions of sandstone above (fine arrows), in context amid other sandstone protrusions; **(b)** ground cross-section showing widening vertical sandstone feature (wide arrow) with horizontal branches penetrating into laminae (grey arrow), and a fine zigzag structure (fine arrow); **(c)** ground cross-section showing narrow, extended vertical disturbance, with vertically displaced laminae in some parts (1), but not in others (2), and fragments of laminae extending along the line of disturbance (3). The disturbance culminates at the top surface in a small sand volcano (4); **(d)** ground cross-section showing disrupted laminae and craters on top surface (arrowed), one with fine sandstone column within; **(e)** view of top surface of block in (d), showing small craters with dark sandstone within. Scale bars: 1 mm.

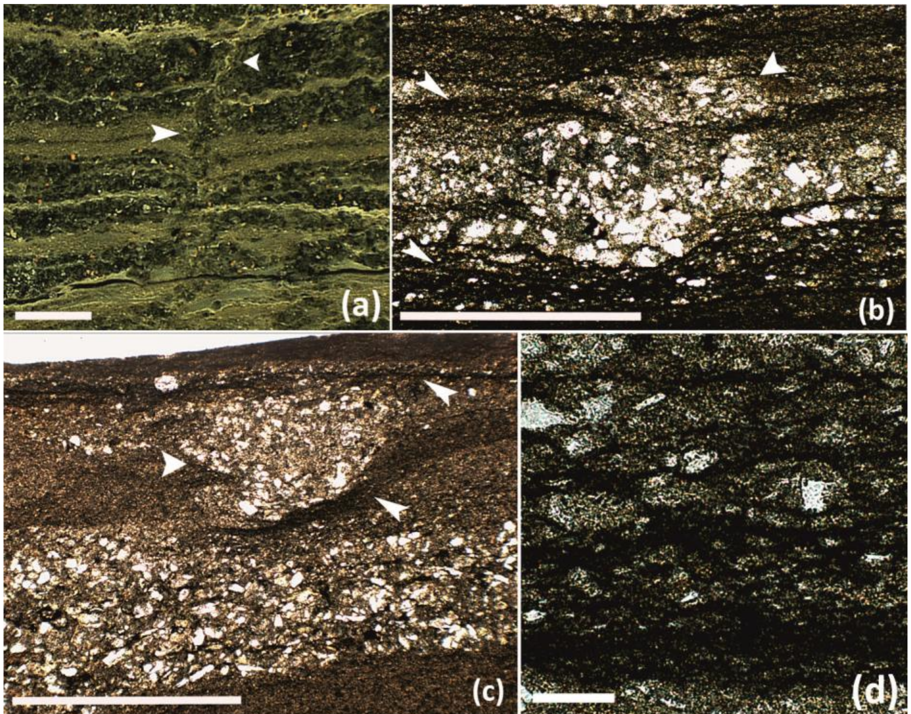

Fig. 4. Microbial mats in cross-section. **(a)** Ground cross-section showing crinkly laminae surrounding a vertical disturbance (disturbance indicated with fine arrow). Note fragments of white lamina extending upwards along the disturbance (wide arrow); **(b** and **c)** photomicrographs of thin sections showing microbial mat layers (fine arrows) constraining sandy sediment structures (wide arrows). Note narrow sinuous connection of V-shaped structure in (c) to sandstone lamina below; **(d)** photomicrograph of thin section showing trapping and binding of sediment grains by microbial mat. Scale bars: (a-c), 1 mm; (d), 100 µm.

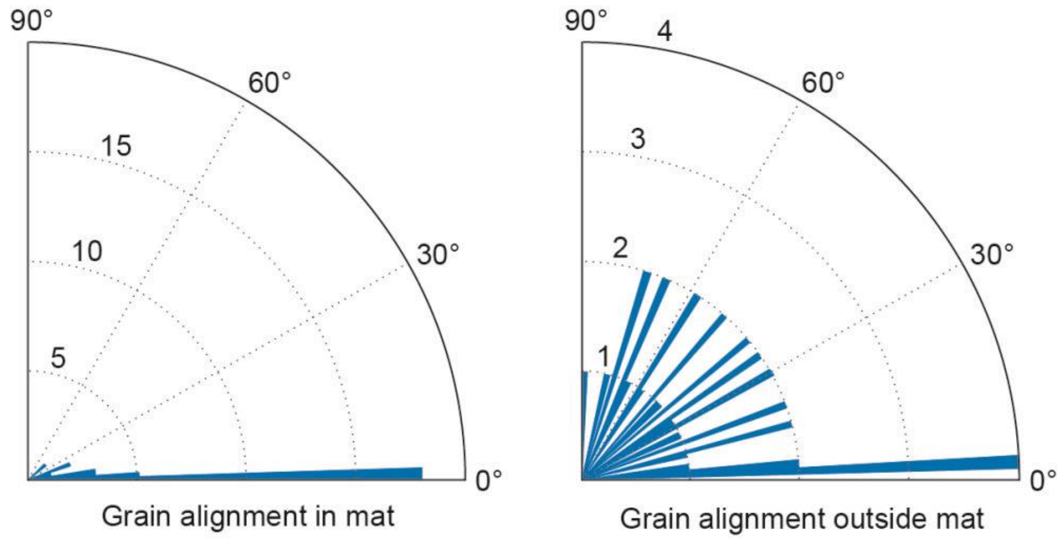

Fig. 5. Comparison of angles of grains trapped in proposed microbial mat (left) compared to those in sandstone layer (right), showing striking grain alignment in the mat layer resulting from trapping and orienting of individual grains within the mat plane by microbes. Total number of grains measured, $N = 40$.

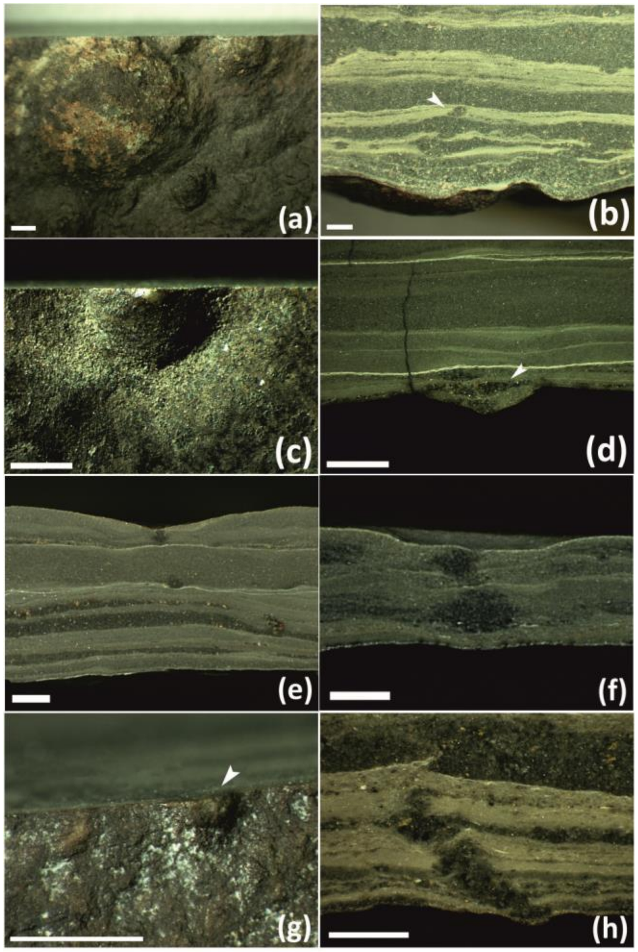

Fig. 6. **(a)** Large and small mound-like *Medusinites* on bed sole before grinding; **(b)** ground cross-section through *Medusinites* shown in (a), illustrating broken and distorted laminae and central oblique sandstone column (arrowed); **(c)** partially ground *Medusinites* with central boss on bed sole; **(d)** ground cross-section through *Medusinites* in (c), showing widening sandstone fill centred on boss (arrowed); **(e** and **f)** ground cross-sections through negative *Medusinites* counterparts on tops of beds, showing sandstone below centre; **(g)**"pimple" or *B. minutae* (arrowed) on bed sole; **(h)** ground cross-section through pimple shown in (g). Scale bars: 1 mm.

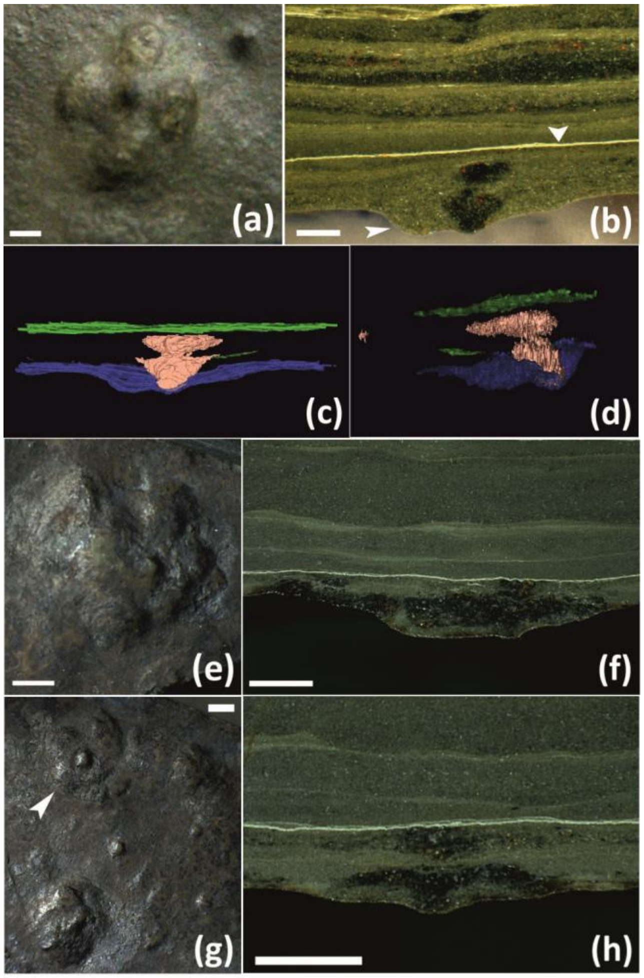

Fig. 7. Lobed *Medusinites* in cross-section. **(a)** Tetra-lobate form with central boss on bed sole, prior to serial grinding; **(b)** ground cross-section through centre of lobate impression in (a), showing dark sand structure centred on boss, and disturbed sediment in surrounding lobes (fine arrow). Note constraining white, crinkly microbial layer above (wide arrow); **(c** and **d)** digital 3D model of specimen created using SPIERS software package (Sutton et al., 2012). Green = white marker horizon seen in (b); blue = basal surface of block, showing disc outline; pink = dark sediment centred on the lobate impression; **(e)** irregular lobed form with five lobes on bed sole, abutted against mound; **(f)** ground cross-section through lobate form shown in (e); **(g)** several *Medusinites* showing lobate tendency, together with isolated pimples, on bed sole; **(h)** ground cross-section through arrowed *Medusinites* with poorly formed lobes in (g). Compare with cross-section through well-formed lobate impression shown in (b). Scale bars: 1 mm.

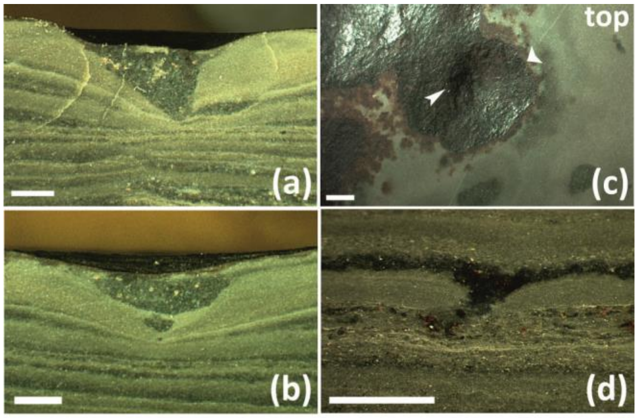

Fig. 8. (a and **b)** Ground cross-sections through shallow, rimless depressions (Longmyndian *B. brunsae*), showing conical sandstone structures in laminae just below top surface. Note distortion of laminae surrounding cone; **(c)** grinding of top surface parallel to bedding reveals wide top of cone (wide arrow) directly below, resulting from sill-like spread of sandy sediment. Note central dip in top of cone (fine arrow), and also small round dark patches to bottom and right of picture, being cross-sections through vertical sand columns; **(d)** similar conical structures observed within ground cross-sections through blocks show cone extending as fine column and often linking to a lower sandstone bed. Note dip in centre of top of cone. Scale bars: 1 mm.

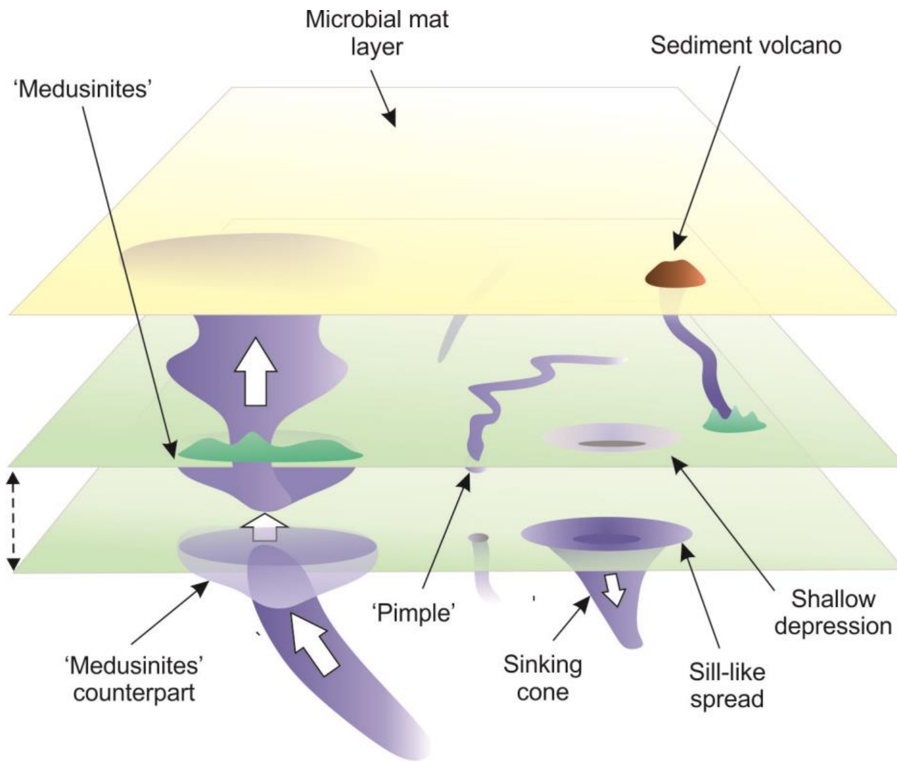

Fig. 9. Schematic 3D representation of proposed model for formation of *Medusinites*-like forms and shallow depressions in the upper Burway Formation. Exploded view of two contiguous surfaces at the bottom of the diagram (dashed arrows) shows markings on sole of bed and counterparts on top of lamina below. To left, "Medusinites" feature is formed by injection and spread of sand slurry, resulting in displacement and loading of sediment. To right, shallow, *B. brunsae*-like depression is produced by sinking, through loading, of a conical sand body in lamina directly below. Formation of smaller scale "pimple" ("B. minutae") and sediment volcano are also shown.

393

394